

Photo-induced charge-transfer renormalization in NiO

Tobias Lojewski,¹ Denis Golež,^{2,3} Katharina Ollefs,¹ Loïc Le Guyader,⁴ Lea Kämmerer,¹ Nico Rothenbach,¹ Robin Y. Engel,⁵ Piter S. Miedema,⁵ Martin Beye,^{5,6} Gheorghe S. Chiuzbăian,⁷ Robert Carley,⁴ Rafael Gort,⁴ Benjamin E. Van Kuiken,⁴ Giuseppe Mercurio,⁴ Justina Schlappa,⁴ Alexander Yaroslavtsev,^{4,8} Andreas Scherz,⁴ Florian Döring,⁹ Christian David,⁹ Heiko Wende,¹ Uwe Bovensiepen,^{1,10} Martin Eckstein,¹¹ Philipp Werner,¹² and Andrea Eschenlohr^{1,*}

¹*Faculty of Physics and Center for Nanointegration Duisburg-Essen (CENIDE),
University of Duisburg-Essen, Lotharstr. 1, 47057 Duisburg, Germany*

²*Jozef Stefan Institute, Jamova 39, 1000 Ljubljana, Slovenia*

³*Faculty of Mathematics and Physics, University of Ljubljana, Jadranska 19, 1000 Ljubljana, Slovenia*

⁴*European XFEL, Holzkoppel 4, 22869 Schenefeld, Germany*

⁵*Deutsches Elektronen-Synchrotron DESY, Notkestr. 85, 22607 Hamburg, Germany*

⁶*Department of Physics, AlbaNova University Center,
Stockholm University, SE-10691 Stockholm, Sweden*

⁷*Sorbonne Université, CNRS, Laboratoire de Chimie Physique - Matière et Rayonnement, 75005 Paris, France*

⁸*Department of Physics and Astronomy, Uppsala University, 75120 Uppsala, Sweden*

⁹*Paul Scherrer Institut, Forschungsstr. 111, 5232 Villigen PSI, Switzerland*

¹⁰*Institute for Solid State Physics, The University of Tokyo, Kashiwa, Chiba 277-8581, Japan*

¹¹*I. Institute of Theoretical Physics, University of Hamburg, 20355 Hamburg, Germany*

¹²*Department of Physics, University of Fribourg, 1700 Fribourg, Switzerland*

(Dated: May 27, 2024)

Photo-doped states in strongly correlated charge transfer insulators are characterized by d - d and d - p interactions and the resulting intertwined dynamics of charge excitations and local multiplets. Here we use femtosecond x-ray absorption spectroscopy in combination with dynamical mean-field theory to disentangle these contributions in NiO. Upon resonant optical excitation across the charge transfer gap, the Ni L_3 and O K absorption edges red-shift for > 10 ps, associated with photo-induced changes in the screening environment. An additional signature below the Ni L_3 edge is identified for < 1 ps, reflecting a transient nonthermal population of local many-body multiplets. We employ a nonthermal generalization of the multiplet ligand field theory to show that the feature originates from d - d transitions. Overall, the photo-doped state differs significantly from a chemically doped state. Our results demonstrate the ability to reveal excitation pathways in correlated materials by x-ray spectroscopies, which is relevant for ultrafast materials design.

Strongly correlated materials host some of the most intriguing states of matter due to the competition between interaction-induced localization and the itinerant nature of electrons, and they are therefore ideal candidates to realize material control on ultrafast timescales [1, 2]. Paradigmatic examples are Mott and charge-transfer (CT) insulators, whose optical properties are determined by the charge transfer between the ligand (typically p) and the correlated orbital (typically d) states [3–5]. Element- and site-selective information on many-body states in such materials can be obtained by resonant soft x-ray absorption and emission spectroscopies [6–8] complementing optical spectroscopy [9, 10]. A comparison of core level absorption edges and their fine structure with cluster calculations [11–16] or dynamical mean-field theory (DMFT) [17–19] can provide detailed information about the CT gap, Coulomb repulsion [11, 20–22], d - d multiplet excitations [7, 23], and the hybridization between the ligand and correlated orbitals [24, 25]. Furthermore, ligand absorption edges probe the itinerant states [24], whose nature is crucial for understanding the

low-energy physics in chemically doped systems [26–28].

Femtosecond time-resolved x-ray spectroscopy is sensitive to low energy excitations and transient energy shifts [29–34]. It is, thus, a potentially powerful tool for investigating photo-excited non-equilibrium states in Mott and CT insulators. Recently, a strong sub-gap excitation has been shown to modify the gap size during the pulse both in cuprate [35] and nickelate [36, 37] CT insulators. These effects can be attributed to photo-manipulations of the screening environment [35], the magnetic order [36], or the hybridization between correlated and itinerant orbitals [37], coined dynamical Franz-Keldysh effect [38]. A natural open question is how this picture changes in the case of resonant excitations, which create long-lived charge carriers in the conduction band, and lead to so-called photo-doped states which may host various non-trivial quantum phases [39–42]. To understand these states, and to potentially design targeted excitation pathways, it is important to clarify the different nature of the charge carriers in photo-doped and chemically doped states, and to disentangle effects such as band shifts due to dynamical screening [43, 44] and charge redistribution between orbitals [43, 45–47] from the dynamics of Mott excitons or electronic d - d excitations [48–51].

* andrea.eschenlohr@uni-due.de

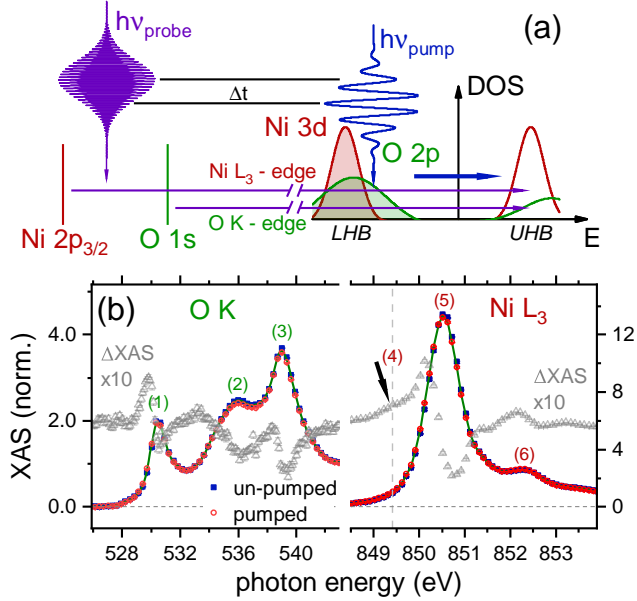


FIG. 1. (a) Transitions by the optical pump $h\nu_{\text{pump}}$ and the x-ray probe $h\nu_{\text{probe}}$ which is delayed by Δt . (b) Ground state (blue squares) and pumped (red circles) XAS at the O K (left) and Ni L_3 edges (right) for $\Delta t = 0.5$ ps and 4 mJ/cm^2 fluence. The pumped XAS are modeled based on the static XAS (green line), see [52]. The gray data show the pump-induced difference ΔXAS vertically offset.

In this Letter, we demonstrate for the paradigmatic CT insulator NiO how time-resolved x-ray absorption spectroscopy (tr-XAS) combined with non-equilibrium dynamical mean-field theory (DMFT) [53, 54] can provide exactly this information upon resonant pumping. We identify energy shifts and lineshape modifications in the excitonic peaks at the Ni L_3 and O K absorption edges, and link them to orbital occupations and the screening environment. In addition, we resolve a short-lived Ni L_3 pre-edge feature that represents many-body multiplets, i.e. $d-d$ excitations, as confirmed by the non-thermal generalization of multiplet ligand field theory.

Figure 1(a) shows a sketch of tr-XAS at the Ni L_3 ($2p_{3/2} \rightarrow 3d$) and O K ($1s \rightarrow 2p$) edges. The experiments were performed at room temperature at the Spectroscopy and Coherent Scattering (SCS) instrument of European XFEL using a pump-probe setup with an effective time resolution of 80 fs [34, 55, 56]. Laser pulses with 4.7 eV photon energy, 35 fs pulse duration, and $0.8\text{-}4 \text{ mJ/cm}^2$ incident fluence were employed to pump 37 nm thick polycrystalline NiO films [52] above the CT gap. This pumping involves excitations from the O $2p$ states to the upper Hubbard band (UHB) [50], see Fig. 1(a). Figure 1(b) depicts the O K and Ni L_3 XAS signals before and after photoexcitation at a pump-probe delay of $\Delta t = 0.5$ ps, with the pump-induced difference ΔXAS shown by the gray dots. We find a spectral shift of all features, labeled

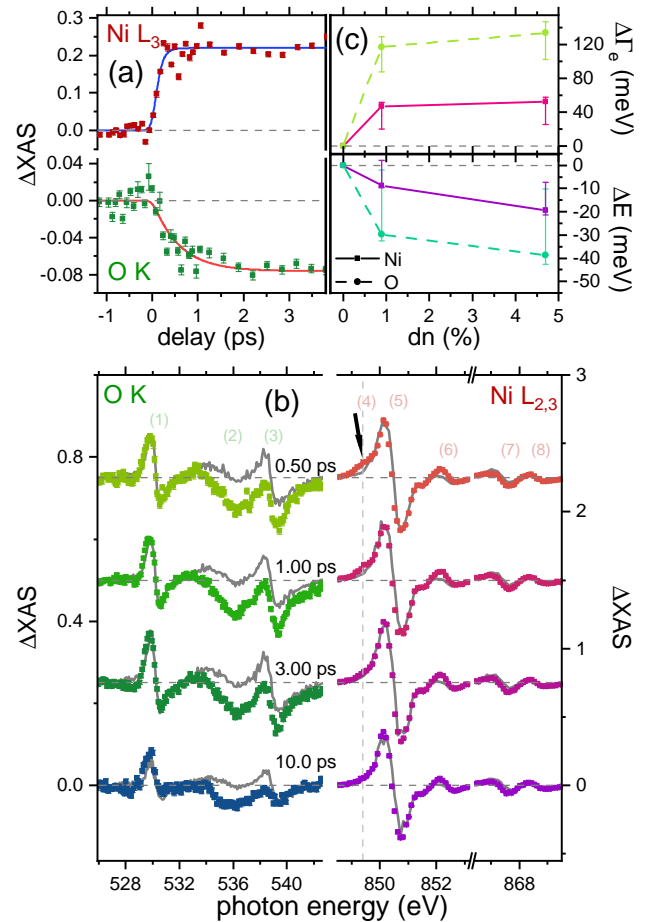


FIG. 2. (a) Time-dependence of ΔXAS for photon energy 539.15 eV (O K) and 850.15 eV (Ni L_3), with exponential fits (lines), for the excited charge carrier density $dn = 4.7\%$ (see [52] for the determination). (b) ΔXAS at the O K and Ni L_3 edges for 4 mJ/cm^2 fluence at the indicated Δt and offset vertically. The gray lines show results obtained by a shift ΔE and broadening $\Delta\Gamma$ of the static spectra, see [52]. The best fit is used to determine these two parameters. (c) ΔE and $\Delta\Gamma$ at the O K and Ni L_3 edges from fits in (b) as a function of dn determined at $\Delta t = 0.5$ ps.

as (1)-(6), to lower x-ray photon energies, as indicated by the derivative-like shape of ΔXAS . We also measured the time dependence at fixed photon energies at both edges, see Fig. 2(a). Exponential fits to these transients, convoluted with 80 fs time resolution [34], indicate a rise time of 99 ± 20 fs for 4.0 mJ/cm^2 pump fluence at the Ni L_3 edge and 580 ± 140 fs at the O K edge. These energy shifts build up, reach a plateau within 2 ps, and decay on longer timescales. This is in contrast to previous tr-XAS on NiO upon subgap pumping, which showed (smaller) modifications only during the pulse [36, 37]. We attribute the difference to the presence of long-lived holon-doublon pairs after the above-gap excitation. These cannot recombine due to the kinetic constraints [57-59] and modify the screening environment [60, 61].

In a first analysis we compare the spectra of the photo-excited system to curves modelled by a red-shift ΔE and a broadening $\Delta\Gamma$ of the static spectra, c.f. Fig. 2(b). In Fig. 2(c) we plot the best fit ΔE and $\Delta\Gamma$ at $\Delta t = 0.5$ ps as a function of the excitation density dn , i.e., the density of pump-excited electrons relative to all valence electrons (see [52] for the determination of dn). The changes in the broadening (or, since $\Gamma \propto 1/\tau$, the changes in the lifetime) are larger for the itinerant p than for the d electrons [34, 52]. Such transient spectral broadening was previously shown to result from lattice excitation [31, 62]. We thus conclude that lattice excitation, most likely trapping of photo-doped charge carriers by polaron formation [63, 64] found on few ps timescales in NiO [65], contributes to the long lifetime of the photoexcited state.

While some parts of the spectrum can be reproduced by the shift and broadening, there are important differences: These include parts of the O K spectrum around 536 eV, as well as an additional pump-induced feature in the pre-edge region of the Ni L_3 edge (see vertical arrow in Fig. 2(b)), which decays within less than 3 ps.

In the following, we will consider the electronic contribution to the bandgap renormalization and comment on possible polaronic contributions at the end. The red-shift is a generic consequence of photo-doping in CT insulators, which arises simultaneously from (i) dynamical screening of the Coulomb interaction parameters on the transition metal site, and (ii) nonlocal Coulomb interactions between photo-doped ligand holes and electrons in the core and valence orbitals (Hartree shift) [38, 43, 44]. As a first illustration, consider a simple cluster consisting of a valence (d), core (c), and ligand (p) orbital, with density-density Coulomb interactions $U_{dd}, U_{cd}, U_{pd}, U_{cp}$, but no p - d hybridization. Upon photo-excitation, the XAS energy for the transition from the core level to the valence d level will shift like $\Delta E_{\text{XAS}} = [\Delta U_{dd} + \Delta\epsilon_d - \Delta\epsilon_c - \Delta U_{cd}] + [\Delta N_p(U_{pd} - U_{cp})]$; here the first square bracket represents the change of the local interactions (U_{dd}, U_{cd}) and level positions (ϵ_d, ϵ_c) by modified screening [43, 44], while the second term is a Hartree shift due to the addition of ligand holes ($\Delta N_p = N_p - N_p^{(0)}$ is the change in the total ligand occupation).

To demonstrate that such Coulomb shifts prevail beyond the simplistic atomic model, we perform a lattice simulation which includes both a microscopic description of dynamical screening and Hartree shifts. We employ a minimal model for a CT insulator, including one transition metal d orbital and two oxygen p orbitals per unit cell. The hopping between the d and p orbitals t_{dp} , the crystal-field splitting Δ_{dp} and Coulomb interaction parameters are adjusted to match the equilibrium spectral function of NiO and the only free parameter is U_{cp} , which is typically not considered in equilibrium, see [52] for details. To capture the strong correlations from the Hubbard interaction U_{dd} and the photo-induced changes in screening, we use the GW+DMFT formalism [43, 60, 66]. We simulate the photo-excitation by a time-dependent electric field pulse. The XAS signal is calculated by solv-

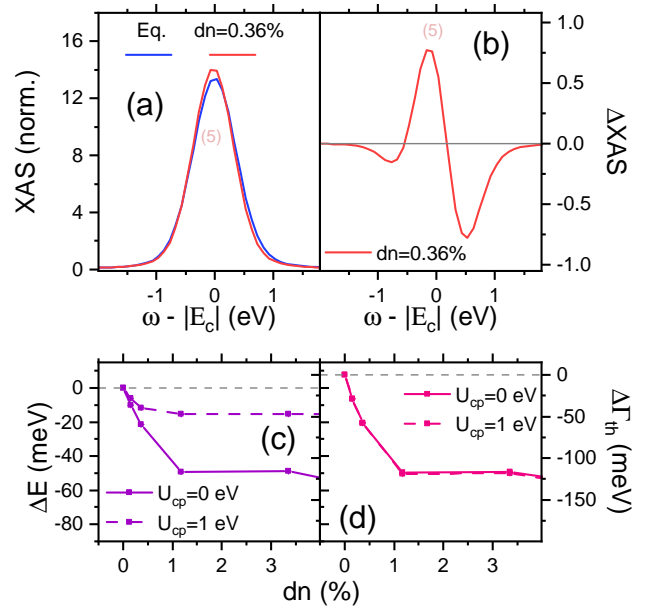


FIG. 3. (a) Calculated equilibrium XAS (blue) and photo-doped XAS (red line) at photo-doping $dn = 0.36\%$ and a delay of $\Delta t = 7$ fs after the pulse, with the photo-induced change ΔXAS in (b). Shift ΔE (c) and lifetime change $\Delta\Gamma$ (d) of the exciton peak versus photo-doping dn determined from the calculations for the given values of the core-oxygen interaction U_{cp} and $U_{dd} = U_{cd} = 7.5$ eV.

ing an auxiliary impurity problem that includes an additional core-level with a lifetime $1/\Gamma$ ($\Gamma = 0.05$ fs $^{-1}$); see [67] for details. X-ray energies are measured relative to the position of the main excitonic resonance $|E_c|$ in the equilibrium spectrum.

In the simulation, the photo-excited charge carriers quickly relax to the edge of the charge-transfer gap and are then trapped due to kinetic constraints. While the full GW+DMFT simulations are restricted to short times, previous DMFT simulations for a comparable gap demonstrated a long (ps) lifetime of the photo-doped charge carriers [68]. We therefore expect that also the XAS signal will not change much on this scale, and can be compared to the long-lived experimental signal in the photo-doped state. The results in Fig. 3 confirm an almost rigid red-shift of the XAS line after photo-doping. The relative importance of the Hartree shift and dynamical screening does not affect this qualitative behavior, but only the magnitude of the shift (compare in Fig. 3(c) the results for $U_{cp} = U_{pd} = 1$ eV, for which the Hartree shifts in the atomic model cancel, and those for $U_{cp} = 0$). This indicates that the Coulomb shift of the XAS exciton is a generic feature of photo-doped systems, which arises jointly from the dynamical screening of the local interactions and Hartree shifts. Polaronic effects (stretching of the Ni-O distance) [64] are further candidates for the bandgap renormalization [69, 70] and future improvements in the time resolution should enable a separation

of the electronic and lattice contributions due to their different timescales.

Our calculations show that the redshift increases linearly with the photo-doping density and then saturates (Fig. 3c), which is in agreement with the experiment (Fig. 2(c)). A notable difference to the experiment is that the spectra in the simulations do not broaden but become even more narrow (c.f. Fig. 1(a) and Fig. 3(a)). This may be because the simulation does not capture additional scattering channels, which can lead to a change of the lineshape of the exciton, such as lattice (polaron) [64] fluctuations.

An interesting question is whether time-resolved XAS can disentangle the different contributions to the Coulomb shift. Assuming a cancellation of the Hartree shifts ($U_{cp} = U_{pd}$) and no screening of U_{cd} , ΔXAS would measure the change of the Hubbard interaction ΔU_{dd} , as concluded previously [35]. However, the observed energy shifts (see Fig. 2(c)) of less than 100 meV are small compared to the interaction parameters, so that a statement on the detailed origin of the shift would require precise knowledge of U_{dd} , U_{cd} , U_{pd} and U_{cp} , which is beyond the capability of current first principles approaches such as constrained RPA [71]. These difficulties prevent a clear quantification of the relative importance of Hartree shifts and dynamical screening and we expect that both contributions are significant. Nevertheless, our analysis proves a high sensitivity of ΔXAS to the microscopic interactions and therefore shows that time-resolved XAS can give information on various Coulomb parameters (and their changes upon photo-doping) that is not easily obtained otherwise, including the nonlocal terms U_{pd} and U_{cp} which are often neglected even in equilibrium [6, 20].

Having interpreted the red shift of the L_3 edge, we now focus on the transient pre-edge feature in the Ni L_3 ΔXAS at $\Delta t = 0.25$ ps (Fig. 4(a)), which is absent at the longest delay times (see Fig. 2(b)). This motivates an analysis of the multiplet structure of NiO beyond our simple charge-transfer insulator model. Ref. [67] showed that the positions of the excitonic resonances in the XAS signal of photo-excited systems within time-dependent DMFT can be well reproduced by atomic limit calculations and that their relative amplitudes in the full many-body state on the lattice allow to measure the time-dependent weight of the different local multiplets. This observation motivates us to generalize the multiplet ligand theory [15] to nonthermal distributions [72]. We follow the standard procedure and define an extended Anderson impurity problem, starting from the DFT electronic structure [17, 25]. Note that we employ the nonthermal occupations $\rho_{ii}[\alpha_a] = \frac{\rho_{ii}^{th} + \alpha_a \delta_{ia}}{\text{Tr}[\rho_{ii}^{th} + \alpha_a \delta_{ia}]}$ with α_a representing the extra weight for the a -th eigenstate. These calculations were performed using the EDRIXS library [73], include the full d shell as well as the ligand bands, and they allow us to distinguish between photo-induced $d-d$ transitions and charge transfer excitations, in contrast to earlier cluster studies [11, 12].

We first discuss the photo-induced difference be-

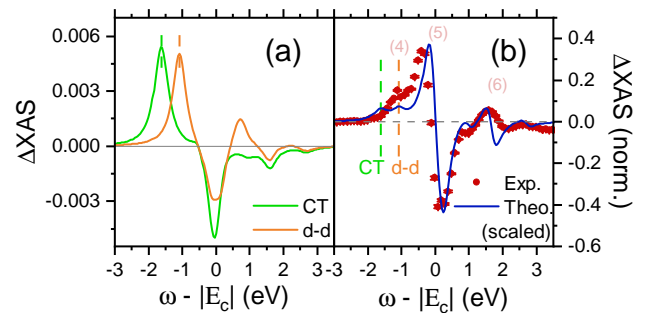


FIG. 4. (a) Change $\Delta XAS[\omega, \alpha_a]$ in the XAS signal due to the nonthermal population of a low-lying excited state of predominantly $d-d$ excitation character ($\alpha_3=0.02$) or charge-transfer (CT) character ($\alpha_{12}=0.02$). (b) Comparison of ΔXAS between experiment (Ni L_3 , $\Delta t = 0.25$ ps) and theory for nonthermal orbital populations, with the blue curve scaled to match experiment at transient feature (5). The thermal reference spectrum was calculated for $T = 100$ K.

tween the nonthermal state and the ground state, $\Delta XAS[\omega, \alpha_a] = XAS(\omega, \rho[\alpha_a]) - XAS(\omega, \rho^{th})$, see Fig. 4(a). In the many-body spectrum, there exists a manifold of states around 1 eV above the ground states with a redistribution of electrons within the d shell. We thus attribute them to the $d-d$ excitations, see [52] for a detailed analysis. An excess occupation in these excited states leads to a characteristic modification of the XAS signal, with a pronounced peak appearing below the main resonance (852 eV), a reduction of the spectral weight at the resonance (853 eV) and an additional increase around 854 eV. Even higher up in the spectrum, we identify a charge-transfer excitation [21, 22, 52], which results in a photo-induced peak roughly 0.5 eV lower in energy than the $d-d$ peak. The latter also leads to a reduction of the spectral weight at the excitonic resonance. For a more direct comparison with the experiment, we can combine the effects of screening and the photo-induced changes from the multiplet ligand field theory. Specifically, we consider a rigid band shift of $\omega_{shift} = 50$ meV of the XAS signal and add to it the photoinduced changes associated with two states with $d-d$ and charge-transfer character, $\Delta XAS(\omega) = XAS(\omega) - XAS(\omega + \omega_{shift}) + \sum_{a=3,12} \Delta XAS[\omega, \rho[\alpha_a]]$ where $a = 3, 12$ refers to the states listed in Tab. 1 of [52] and the extra weights are set to $\alpha_a = 2\%$. We have checked that different choices for the nonthermal populations lead to qualitatively similar results. The comparison with the experiment shows an excellent agreement in the photo-renormalized XAS signal below and above the main excitonic resonance.

A comparison of photo- and chemical doping is instructive. Chemical doping leads to the appearance of a pre-edge feature at the O K edge [74] while such a pre-edge peak is absent at the Ni $L_{3,2}$ edges [75]. Photo-doping produces the opposite result, i.e., the absence of a pre-edge feature at the O K edge (which by comparison to

[74] would be expected at 527 eV), and the presence of such a feature at the Ni L_3 edge. The difference between chemically doped and photo-doped spectra is a key observation which shows that photo-doped holes differ in nature from chemically doped holes: They might occupy different p - d hybrid orbitals (such as non-bonding configurations instead of the Zhang-Rice doublet [28]), or there may exist excitonic correlations between photo-doped electrons and holes.

In conclusion, we showed that photo-doping by above charge-transfer gap excitations in NiO results in characteristic transient signatures in XAS. These are (i) energy shifts of the excitonic peaks of several 10 meV for photo-doping on the order of 1%, which persist for tens of ps due to the long lifetime of the photo-doped state and are potentially enhanced by polaronic effects [63, 65, 72], and (ii) many-body multiplet excitations in the Ni L_3 pre-edge region. The good qualitative agreement between the tr-XAS measurements and a simple model for charge-transfer insulators demonstrates that energy shifts resulting from photo-induced changes in the electrostatic Hartree energy are a generic feature in transition metal oxides. Screening-induced changes in the interaction strengths play a role in determining these shifts. Our work furthermore establishes that tr-XAS of photo-excited states is sensitive to the interaction be-

tween core electrons and ligand holes, which is important for a quantitative interpretation of the spectral changes. All these observations reveal generic signatures of charge-transfer insulators, providing a basis for a future systematic analysis of these microscopic phenomena in this important material class, e.g. through the application of sum rules. Disentangling non-equilibrium multiplet effects from time-dependent renormalization of interaction parameters and Hartree shifts further promises to aid the design of tailored excitation protocols for reaching specific photo-doped states.

We acknowledge European XFEL in Schenefeld, Germany, for provision of X-ray free-electron laser beamtime at the SCS instrument and thank the staff for their assistance. Funded by the Deutsche Forschungsgemeinschaft (DFG, German Research Foundation) through Project No. 278162697 - SFB 1242. UB, PW, and ME acknowledge support from the Deutsche Forschungsgemeinschaft (DFG, German Science Foundation) through FOR 5249-449872909 (Project P6). D.G. acknowledges the support by the program No. P1-0044, No. J1-2455 and MN-0016-106 of the Slovenian Research Agency (ARRS).

T. L. performed the experiments and analyzed the data. D. G. did the calculations. Both contributed equally to this work.

-
- [1] C. Giannetti, M. Capone, D. Fausti, M. Fabrizio, F. Parmigiani, and D. Mihailovic, *Advances in Physics* **65**, 58 (2016).
- [2] A. de la Torre, D. M. Kennes, M. Claassen, S. Gerber, J. W. McIver, and M. A. Sentef, *Rev. Mod. Phys.* **93**, 041002 (2021).
- [3] G. A. Sawatzky and J. W. Allen, *Phys. Rev. Lett.* **53**, 2339 (1984).
- [4] J. Zaanen, G. A. Sawatzky, and J. W. Allen, *Phys. Rev. Lett.* **55**, 418 (1985).
- [5] J. Zaanen, C. Westra, and G. A. Sawatzky, *Phys. Rev. B* **33**, 8060 (1986).
- [6] F. M. de Groot, H. Elnaggar, F. Frati, R.-p. Wang, M. U. Delgado-Jaime, M. van Veenendaal, J. Fernandez-Rodriguez, M. W. Haverkort, R. J. Green, G. van der Laan, Y. Kvashnin, A. Hariki, H. Ikeno, H. Ramanantoina, C. Daul, B. Delley, M. Odellius, M. Lundberg, O. Kuhn, S. I. Bokarev, E. Shirley, J. Vinson, K. Gilmore, M. Stener, G. Fronzoni, P. Decleva, P. Kruger, M. Retsgan, Y. Joly, C. Vorwerk, C. Draxl, J. Rehr, and A. Tanaka, *Journal of Electron Spectroscopy and Related Phenomena* **249**, 147061 (2021).
- [7] L. J. Ament, M. Van Veenendaal, T. P. Devereaux, J. P. Hill, and J. Van Den Brink, *Reviews of Modern Physics* **83**, 705 (2011).
- [8] C. Y. Kuo, T. Haupricht, J. Weinen, H. Wu, K. D. Tsuei, M. Haverkort, A. Tanaka, and L. Tjeng, *The European Physical Journal Special Topics* **226**, 2445 (2017).
- [9] R. Newman and R. M. Chrenko, *Phys. Rev.* **114**, 1507 (1959).
- [10] R. Powell and W. Spicer, *Physical Review B* **2**, 2182 (1970).
- [11] G. van der Laan, J. Zaanen, G. A. Sawatzky, R. Karnatak, and J.-M. Esteve, *Phys. Rev. B* **33**, 4253 (1986).
- [12] G. van der Laan, B. T. Thole, G. A. Sawatzky, and M. Verdaguer, *Phys. Rev. B* **37**, 6587 (1988).
- [13] F. de Groot, *Journal of Electron Spectroscopy and Related Phenomena* **62**, 111 (1993).
- [14] A. Tanaka and T. Jo, *Journal of the Physical Society of Japan* **63**, 2788 (1994).
- [15] M. W. Haverkort, M. Zwierzycki, and O. K. Andersen, *Phys. Rev. B* **85**, 165113 (2012).
- [16] O. Šipr, J. Minár, A. Scherz, H. Wende, and H. Ebert, *Phys. Rev. B* **84**, 115102 (2011).
- [17] M. Haverkort, G. Sangiovanni, P. Hansmann, A. Toschi, Y. Lu, and S. Macke, *EPL (Europhysics Letters)* **108**, 57004 (2014).
- [18] P. Cornaglia and A. Georges, *Physical Review B* **75**, 115112 (2007).
- [19] A. Hariki, T. Uozumi, and J. Kuneš, *Phys. Rev. B* **96**, 045111 (2017).
- [20] K. Okada and A. Kotani, *Journal of the Physical Society of Japan* **66**, 341 (1997).
- [21] S. Agrestini, K. Chen, C.-Y. Kuo, L. Zhao, H.-J. Lin, C.-T. Chen, A. Rogalev, P. Ohresser, T.-S. Chan, S.-C. Weng, G. Auffermann, A. Völzke, A. C. Komarek, K. Yamaura, M. W. Haverkort, Z. Hu, and L. H. Tjeng, *Phys. Rev. B* **100**, 014443 (2019).
- [22] T. Burnus, Z. Hu, H. H. Hsieh, V. L. J. Joly, P. A. Joy, M. W. Haverkort, H. Wu, A. Tanaka, H.-J. Lin, C. T. Chen, and L. H. Tjeng, *Phys. Rev. B* **77**, 125124 (2008).
- [23] M. Rossi, H. Lu, A. Nag, D. Li, M. Osada, K. Lee, B. Y.

- Wang, S. Agrestini, M. Garcia-Fernandez, J. J. Kas, Y.-D. Chuang, Z. X. Shen, H. Y. Hwang, B. Moritz, K.-J. Zhou, T. P. Devereaux, and W. S. Lee, *Phys. Rev. B* **104**, L220505 (2021).
- [24] T. M. Schuler, D. L. Ederer, S. Itza-Ortiz, G. T. Woods, T. A. Callcott, and J. C. Woicik, *Phys. Rev. B* **71**, 115113 (2005).
- [25] J. Lüder, J. Schött, B. Brena, M. W. Haverkort, P. Thunström, O. Eriksson, B. Sanyal, I. Di Marco, and Y. O. Kvashnin, *Physical Review B* **96**, 245131 (2017).
- [26] M. Taguchi, M. Matsunami, Y. Ishida, R. Eguchi, A. Chainani, Y. Takata, M. Yabashi, K. Tamasaku, Y. Nishino, T. Ishikawa, Y. Senba, H. Ohashi, and S. Shin, *Phys. Rev. Lett.* **100**, 206401 (2008).
- [27] J. Kuneš, V. Anisimov, A. Lukoyanov, and D. Vollhardt, *Physical Review B* **75**, 165115 (2007).
- [28] J. Bala, A. M. Oleś, and J. Zaanen, *Physical review letters* **72**, 2600 (1994).
- [29] C. Stamm, N. Pontius, T. Kachel, M. Wietstruk, and H. A. Dürr, *Phys. Rev. B* **81**, 104425 (2010).
- [30] A. D. Smith, T. Balčiunas, Y.-P. Chang, C. Schmidt, K. Zinchenko, F. B. Nunes, E. Rossi, V. Svoboda, Z. Yin, J.-P. Wolf, and H. J. Wörner, *J. Phys. Chem. Lett.* **11**, 1981 (2020).
- [31] N. Rothenbach, M. E. Gruner, K. Ollefs, C. Schmitz-Antoniak, S. Salamon, P. Zhou, R. Li, M. Mo, S. Park, X. Shen, S. Weathersby, J. Yang, X. J. Wang, R. Pentcheva, H. Wende, U. Bovensiepen, K. Sokolowski-Tinten, and A. Eschenlohr, *Phys. Rev. B* **100**, 174301 (2019).
- [32] E. Diesen, H.-Y. Wang, S. Schreck, M. Weston, H. Ogasawara, J. LaRue, F. Perakis, M. Dell'Angela, F. Capotondi, L. Giannessi, E. Pedersoli, D. Naumenko, I. Nikolov, L. Raimondi, C. Spezzani, M. Beye, F. Cavalca, B. Liu, J. Gladh, S. Koroidov, P. S. Miedema, R. Costantini, T. F. Heinz, F. Abild-Pedersen, J. Voss, A. C. Luntz, and A. Nilsson, *Phys. Rev. Lett.* **127**, 016802 (2021).
- [33] T. P. H. Sidiropoulos, N. Di Palo, D. E. Rivas, S. Severino, M. Reduzzi, B. Nandy, B. Bauerhenne, S. Krylow, T. Vasileiadis, T. Danz, P. Elliott, S. Sharma, K. Dewhurst, C. Ropers, Y. Joly, M. E. Garcia, M. Wolf, R. Ernstorfer, and J. Biegert, *Phys. Rev. X* **11**, 041060 (2021).
- [34] T. Lojewski, M. F. Elhanoty, L. L. Guyader, O. Grånäs, N. Agarwal, C. Boeglin, R. Carley, A. Castoldi, C. David, C. Deiter, F. Döring, R. Engel, F. Erdinger, H. Fangohr, C. Fiorini, P. Fischer, N. Gerasimova, R. Gort, F. de-Groot, K. Hansen, S. Hauf, D. Hickin, M. Izquierdo, B. E. V. Kuiken, Y. Kvashnin, C.-H. Lambert, D. Lomidze, S. Maffessanti, L. Mercadier, G. Mercurio, P. S. Miedema, K. Ollefs, M. Pace, M. Porro, J. Rezvani, B. Rösner, N. Rothenbach, A. Samartsev, A. Scherz, J. Schlappa, C. Stamm, M. Teichmann, P. Thunström, M. Turcato, A. Yaroslavtsev, J. Zhu, M. Beye, H. Wende, U. Bovensiepen, O. Eriksson, and A. Eschenlohr, *Mater. Res. Lett.* **11**, 655 (2023).
- [35] D. R. Baykusheva, H. Jang, A. A. Husain, S. Lee, S. F. R. TenHuisen, P. Zhou, S. Park, H. Kim, J.-K. Kim, H.-D. Kim, M. Kim, S.-Y. Park, P. Abbamonte, B. J. Kim, G. D. Gu, Y. Wang, and M. Mitran, *Phys. Rev. X* **12**, 011013 (2022).
- [36] X. Wang, R. Y. Engel, I. Vaskivskiy, D. Turenne, V. Shokeen, A. Yaroslavtsev, O. Grånäs, R. Knut, J. O. Schunck, S. Dziarzhytski, *et al.*, *Faraday Discussions* **237**, 300 (2022).
- [37] O. Grånäs, I. Vaskivskiy, X. Wang, P. Thunström, S. Ghimire, R. Knut, J. Söderström, L. Kjellsson, D. Turenne, R. Y. Engel, M. Beye, J. Lu, D. J. Higley, A. H. Reid, W. Schlotter, G. Coslovich, M. Hoffmann, G. Kolesov, C. Schüßler-Langeheine, A. Styervoyedov, N. Tancogne-Dejean, M. A. Sentef, D. A. Reis, A. Rubio, S. S. P. Parkin, O. Karis, J.-E. Rubensson, O. Eriksson, and H. A. Dürr, *Phys. Rev. Res.* **4**, L032030 (2022).
- [38] N. Tancogne-Dejean, M. A. Sentef, and A. Rubio, *Phys. Rev. B* **102**, 115106 (2020).
- [39] L. Stojchevska, I. Vaskivskiy, T. Mertelj, P. Kusar, D. Svetin, S. Brazovskii, and D. Mihailovic, *Science* **344**, 177 (2014).
- [40] J. Li, H. U. R. Strand, P. Werner, and M. Eckstein, *Nat. Commun.* **9**, 4581 (2018).
- [41] T. Kaneko, T. Shirakawa, S. Sorella, and S. Yunoki, *Phys. Rev. Lett.* **122**, 077002 (2019).
- [42] J. Li, D. Golez, P. Werner, and M. Eckstein, *Mod. Phys. Lett. B* **34**, 2040054 (2020).
- [43] D. Golež, L. Boehnke, M. Eckstein, and P. Werner, *Phys. Rev. B* **100**, 041111 (2019).
- [44] N. Tancogne-Dejean, M. A. Sentef, and A. Rubio, *Phys. Rev. Lett.* **121**, 097402 (2018).
- [45] M. Sandri and M. Fabrizio, *Phys. Rev. B* **91**, 115102 (2015).
- [46] Z. He and A. J. Millis, *Phys. Rev. B* **93**, 115126 (2016).
- [47] S. Beaulieu, S. Dong, N. Tancogne-Dejean, M. Dendzik, T. Pincelli, J. Maklar, R. P. Xian, M. A. Sentef, M. Wolf, A. Rubio, *et al.*, *Science Advances* **7**, eabd9275 (2021).
- [48] H. U. R. Strand, D. Golež, M. Eckstein, and P. Werner, *Phys. Rev. B* **96**, 165104 (2017).
- [49] J. Rincón, E. Dagotto, and A. E. Feiguin, *Phys. Rev. B* **97**, 235104 (2018).
- [50] K. Gillmeister, D. Golez, C.-T. Chiang, N. Bittner, Y. Pavlyukh, J. Berakdar, P. Werner, and W. Widdra, *Nature Communications* **11**, 4095 (2020).
- [51] A. Müller, F. Grandi, and M. Eckstein, *Phys. Rev. B* **106**, L121107 (2022).
- [52] See the supplement for the calculation of the excitation density and more information on sample preparation and characterization, data processing, background removal, our criteria to exclude effects due to sample damage, the modelling to extract spectral shifts and broadening, and the theoretical method.
- [53] A. Georges, G. Kotliar, W. Krauth, and M. J. Rozenberg, *Rev. Mod. Phys.* **68**, 13 (1996).
- [54] H. Aoki, N. Tsuji, M. Eckstein, M. Kollar, T. Oka, and P. Werner, *Rev. Mod. Phys.* **86**, 779 (2014).
- [55] L. Le Guyader, A. Eschenlohr, M. Beye, W. Schlotter, F. Döring, C. Carinan, D. Hickin, N. Agarwal, C. Boeglin, U. Bovensiepen, J. Buck, R. Carley, A. Castoldi, A. D'Elia, J.-T. Delitz, W. Ehsan, R. Engel, F. Erdinger, H. Fangohr, P. Fischer, C. Fiorini, A. Föhlisch, L. Gelisio, M. Gensch, N. Gerasimova, R. Gort, K. Hansen, S. Hauf, M. Izquierdo, E. Jal, E. Kamil, S. Karabekyan, T. Kluyver, T. Laarmann, T. Lojewski, D. Lomidze, S. Maffessanti, T. Mamyrbayev, A. Marcelli, L. Mercadier, G. Mercurio, P. S. Miedema, K. Ollefs, K. Rossnagel, B. Rösner, N. Rothenbach, A. Samartsev, J. Schlappa, K. Setoodehnia, G. Sorin Chiuzaibaian, L. Spieker, C. Stamm, F. Stellato, S. Techert, M. Teichmann, M. Turcato, B. Van Kuiken,

- H. Wende, A. Yaroslavtsev, J. Zhu, S. Molodtsov, C. David, M. Porro, and A. Scherz, *Journal of Synchrotron Radiation* **30**, 284 (2023).
- [56] Data recorded for the experiment at the European XFEL are available at doi:10.22003/xfel.eu-data-002589-00.
- [57] Y. Murakami, D. Golež, M. Eckstein, and P. Werner, Photo-induced nonequilibrium states in Mott insulators (2023), [arXiv:2310.05201 \[cond-mat.str-el\]](https://arxiv.org/abs/2310.05201).
- [58] R. Sensarma, D. Pekker, E. Altman, E. Demler, N. Strohmaier, D. Greif, R. Jördens, L. Tarruell, H. Moritz, and T. Esslinger, *Physical Review B* **82**, 224302 (2010).
- [59] Z. Lenarčič and P. Prelovšek, *Phys. Rev. Lett.* **111**, 016401 (2013).
- [60] D. Golež, L. Boehnke, H. U. R. Strand, M. Eckstein, and P. Werner, *Phys. Rev. Lett.* **118**, 246402 (2017).
- [61] D. Golež, M. Eckstein, and P. Werner, *Phys. Rev. B* **92**, 195123 (2015).
- [62] N. Rothenbach, M. E. Gruner, K. Ollefs, C. Schmitz-Antoniak, S. Salamon, P. Zhou, R. Li, M. Mo, S. Park, X. Shen, S. Weathersby, J. Yang, X. J. Wang, O. Šipr, H. Ebert, K. Sokolowski-Tinten, R. Pentcheva, U. Bovensiepen, A. Eschenlohr, and H. Wende, *Phys. Rev. B* **104**, 144302 (2021).
- [63] R. Karsthof, M. Grundmann, A. M. Anton, and F. Krenner, *Phys. Rev. B* **99**, 235201 (2019).
- [64] D. Ishikawa, M. W. Haverkort, and A. Q. Baron, *Journal of the Physical Society of Japan* **86**, 093706 (2017).
- [65] S. Biswas, J. Husek, S. Londo, and L. R. Baker, *The Journal of Physical Chemistry Letters* **9**, 5047 (2018).
- [66] D. Golež, M. Eckstein, and P. Werner, *Phys. Rev. B* **100**, 235117 (2019).
- [67] P. Werner, D. Golež, and M. Eckstein, *Phys. Rev. B* **106**, 165106 (2022).
- [68] N. Dasari, J. Li, P. Werner, and M. Eckstein, *Phys. Rev. B* **103**, L201116 (2021).
- [69] P. Werner and M. Eckstein, *Europhysics Letters* **109**, 37002 (2015).
- [70] P. Erhart, A. Klein, D. Åberg, and B. Sadigh, *Phys. Rev. B* **90**, 035204 (2014).
- [71] F. Aryasetiawan, M. Imada, A. Georges, G. Kotliar, S. Biermann, and A. I. Lichtenstein, *Phys. Rev. B* **70**, 195104 (2004).
- [72] L. M. Carneiro, S. K. Cushing, C. Liu, Y. Su, P. Yang, A. P. Alivisatos, and S. R. Leone, *Nature materials* **16**, 819 (2017).
- [73] Y. Wang, G. Fabbris, M. Dean, and G. Kotliar, *Computer Physics Communications* **243**, 151 (2019).
- [74] P. Kuiper, G. Kruizinga, J. Ghijsen, G. A. Sawatzky, and H. Verweij, *Phys. Rev. Lett.* **62**, 221 (1989).
- [75] J. van Elp, B. Searle, G. Sawatzky, and M. Sacchi, *Solid State Communications* **80**, 67 (1991).